Space-Borne Passive Location Based on a Virtual Synthetic Aperture Mechanism

Tong Zhang, Qiang Yang, Xin Zhang, and Xiaochuan Wu(✉)

Harbin Institute of Technology, Harbin, China
wxc@hit.edu.cn

Abstract. The passive location method based on space-borne phase interferometer has to design more complex structures of antenna and system to solve the conflict between phase ambiguity and location accuracy. To address the problem, a space-borne passive location method based on virtual aperture is proposed in this paper. This method utilizes the moving characteristics of the space-borne platform to apply the principles of the synthetic aperture into the virtual aperture passive location system to form a new strategy of direction finding and location. We use the equivalent squint range model (ESRM) as the range model and the parameters of the model are estimated by Doppler parameter inversion and geometric approximation. Based on the range model, the received signal is equivalent to a linear frequency modulated signal in the azimuth direction, thus the azimuth location can be completed by matched filtering, while the range location can be completed by range searching. The 2-D coordinates of the radiation source can be obtained by range searching and azimuth focusing.

Keywords: Passive location · Virtual aperture · Range-azimuth location · Space-borne single platform

1 Introduction

Passive location technology has been widely concerned in the decades due to its advantages of low power consumption, long detection distance, good concealment, and strong anti-interference ability [1].

Space-borne passive location systems can be classified as single-satellite passive location systems and multi-satellite passive location systems. Multi-satellite passive location systems have high location accuracy, whose most widely used location methods are time difference of arrival (TDOA), frequency difference of arrival (FDOA), and the joint location method, which have high location accuracy [2–4]. However, it needs to consider issues such as time synchronization and so on, which result in high system complexity and cost. In contrast, although single-satellite passive location systems are not accurate enough, it is widely used because of its low cost and simple system setup.

Traditional single-satellite location systems typically use the direction-finding location method based on the phase interferometer [5] and the location method based on the Doppler frequency [6]. The main problem of the former is phase ambiguity and low location accuracy which have a Coupling Relationship. To improve positioning

Q. Guo et al. (Eds.): WiSATS 2021, LNICST 410, pp. 583–592, 2022.
https://doi.org/10.1007/978-3-030-93398-2_52

accuracy and solve the phase ambiguity problem at the same time, it is often necessary to design more complex systems and antenna structures [7, 8]; The latter mainly uses the change of Doppler frequency generated by the relative movement between the satellite and the target. This location method has lower complexity, but the measurement of Doppler and its change rate is based on the data of different time independently, without using the coherent integration of long-term data [9].

Synthetic aperture radar (SAR) compresses the Doppler signal which is a wideband chirp signal to improve the azimuth resolution. Utilizing the synthetic aperture to passive location, the article [10] proposed a passive location algorithm for radiation sources based on synthetic aperture. However, the feasibility of the method under space-borne conditions and the influence factors of the location error lacked analysis in the article.

On this basis, a space-borne passive location method based on the virtual aperture is proposed in this paper, which uses the equivalent squint range model and obtains the location of radiation source by range searching and azimuth focusing. The parameters of the range model are estimated by the geometric approximation and its Doppler parameters. Besides, the factors which affect the location error such as the length of the virtual aperture and the altitude are analyzed in this paper.

This paper is organized as follows. The signal model under the Equivalent Squint Range Model is presented in Sect. 2. The passive location method and the range model parameters estimation method are presented in Sect. 3. Azimuth resolution, range resolution, and the error caused by the range model are investigated in Sect. 4. Simulation results and the error curves are described in Sect. 5. Finally, the conclusion that the method is practical and the location error is decreasing with the longer synthetic aperture time, the lower orbital altitude and the larger SNR is drawn in Sect. 6.

2 Signal Model

The geometric model of the passive location issues based on the virtual aperture is shown in Fig. 1. While satellite is moving, Equivalent Squint Range Model (ESRM) is a range model for low-orbit space-borne synthetic aperture imaging radar, which is shown in Fig. 2:

$$R(t_a) = \sqrt{R_c^2 + V_r^2 t_a^2 - 2R_c V_r t_a \sin\theta_r} \tag{1}$$

where R_c denotes the range to the target at the center of the beam, V_r denotes the equivalent velocity of the satellite, θ_r denotes the equivalent squint angle, t_a denotes the azimuth time. X_0 in Fig. 2 denotes the azimuth location of the radiation source.

In the case of passive location, assuming that the transmitted signal is a single frequency pulse signal $s(t)$:

$$s(t) = rect(\frac{t}{T_p}) \exp(j2\pi f_c t + \varphi) \tag{2}$$

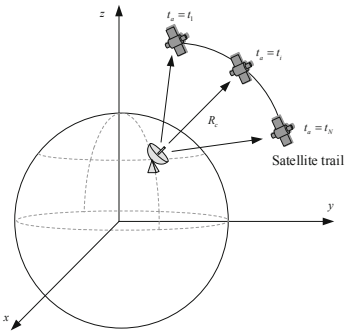

Fig. 1. The geometric model of the passive location

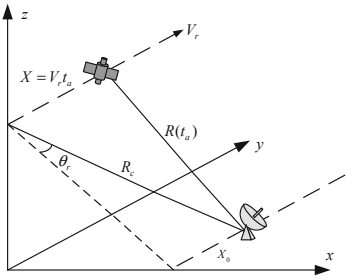

Fig. 2. Equivalent Squint Range Model (ESRM)

where $\text{rect}(u) = \begin{cases} 1 & |u| \le 1/2 \\ 0 & |u| > 1/2 \end{cases}$, f_c is the carrier frequency, φ is the initial phase.

According to the "go-stop-go" model, the received signal can be divided into small pulses of which the pulse width is T_p and the period of each pulse is T. The data utilization mode is shown in Fig. 3. Then rearrange the data into two domains. t_r denotes the range time, $t_a = mT$ denotes the azimuth time, so the time $t = t_r + t_a$.

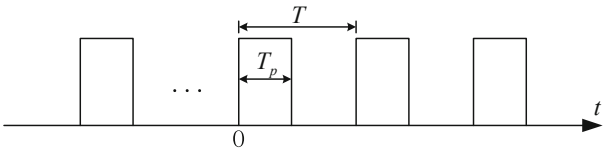

Fig. 3. The data utilization mode

The radiation signal received by at (t_r, t_a) can be represented as:

$$\begin{aligned} s_r(t_r, t_a) &= \text{rect}\left(\frac{t_r}{T_P}\right) \exp\left\{j\left[2\pi f_c\left(t_r + t_a - \frac{R(t_a)}{c}\right) + \varphi\right]\right\} \\ &= \text{rect}\left(\frac{t_r}{T_P}\right) \exp\{\text{j}(2\pi f_c t_r + \varphi)\} \exp\left\{j2\pi f_c\left(t_a - \frac{R(t_a)}{c}\right)\right\} \end{aligned} \tag{3}$$

where the second index term includes the azimuth and range information, so it can be used to locate.

3 Space-Borne Virtual Aperture Location Method

The Fourier expansion omitting cubic and higher-order terms of ESRM is:

$$R(t_a) \approx R_c - V_r \sin\theta_r t_a + \frac{V_r^2 \cos^2\theta_r}{2R_c} t_a^2 \tag{4}$$

Rewrite the received radiation signal (3) as:

$$s_r(t_r, t_a) = K \exp\{j2\pi f_c t_a\} \exp\left\{-j2\pi \frac{f_c}{c}\left(R_c - V_r \sin\theta_r t_a + \frac{V_r^2 \cos^2\theta_r}{2R_c} t_a^2\right)\right\} \tag{5}$$

where $K = \text{rect}\left(\frac{t_r}{T_P}\right) \exp\{\text{j}(2\pi f_c t_r + \varphi)\}$.

The processed signal is a linear frequency modulated (LFM) signal in the slow time domain, the Doppler centroid f_{dc} and Doppler rate f_{1r} are:

$$f_{dc} = \frac{V_r \sin\theta_r}{\lambda} \tag{6}$$

$$f_{1r} = -\frac{V_r^2 \cos^2\theta_r}{\lambda R_c} \tag{7}$$

According to the theory of SAR, the azimuth information can be obtained by matched filtering. The matched filter is:

$$h(t_a) = \exp\left(-j\pi\gamma t_a^2\right) \tag{8}$$

The chirp rate $\gamma = f_{1r}$, where the equivalent velocity of the satellite V_r and the equivalent squint angle θ_r need to be estimated. The traditional parameter estimation method is:

$$V_r \approx \sqrt{V_g V_s} \tag{9}$$

$$\theta_r \approx \frac{V_s}{V_g}\theta_{sq} \tag{10}$$

where V_g is the velocity at which a radar beam moves over the surface, V_s is the velocity of the satellite, θ_{sq} is the oblique view of the radar beam.

However, the above estimation method uses more geometric approximations, which will lead to larger phase errors. To make the model more accurate, we can use the Doppler parameters to estimate V_r and θ_r.

According to (6) and (7), the estimation of V_r and θ_r can be obtained as follows:

$$V_r = \sqrt{(\lambda f_{dc})^2 - \lambda R_c f_{1r}} \tag{11}$$

$$\theta_r = \arcsin(\frac{\lambda f_{dc}}{V_r}) \tag{12}$$

However, because of the passivity, the passive location can't get the range information by matched filtering in the range domain as the SAR, so R_c in (11) is unknown. So the estimation can be obtained via (9) and (12).

As for the location in the range domain, to get the range location R_c, we can use a set of azimuth function with different distances R_k:

$$h(t_a, R_k) = \exp\left(-j\pi\gamma_k t_a^2\right) \tag{13}$$

where $\gamma_k = -\frac{V_r^2 \cos^2\theta_r}{\lambda R_k}$.

The corresponding matched filters can also be constructed directly by using the Principle of Stationary (PSP) in the Doppler domain, f_a denotes the Doppler frequency:

$$H(f_a, R_k) = \exp(j\pi\frac{f_a^2}{\gamma_k}) \tag{14}$$

The received radiation signal is as (5), multiply by $\exp\{-j2\pi f_c t_a\}$ and take the azimuthal Fourier transform of the signal, the Doppler spectrum is:

$$\begin{aligned} W_r(t_r, f_a) &= K' \exp\left\{j\pi\frac{f_a^2}{\gamma}\right\} \exp\left\{-j2\pi f_a \frac{R_c \sin\theta_r}{V_r \cos^2\theta_r}\right\} \\ &= K' \exp\left\{-j2\pi f_a \frac{R_c \sin\theta_r}{V_r \cos^2\theta_r}\right\} H(f_a, R_c) \end{aligned} \tag{15}$$

where $K' = K \exp\left\{-j2\pi\frac{f_c}{c}R_c\right\} \exp\left\{j\pi\frac{\sin^2\theta_r R_c}{\lambda\cos^2\theta_r}\right\}$ is a constant with respect to t_a.

Thus, through the set of matched filters as (16), the output is:

$$\begin{aligned} w(R_k, t_a) &= K' IFFT_{t_a}\{H(f_a, R_c)H(f_a, R_k)\} \otimes \delta\left(t_a - \frac{R_c \sin\theta_r}{V_r \cos^2\theta_r}\right) \\ &\approx K' IFFT_{t_a}\{H(f_a, R_c)H(f_a, R_k)\} \otimes \delta\left(t_a - \frac{X_0}{V_r}\right) \end{aligned} \tag{16}$$

When $R_k = R_c$, the processed signal will be in full focus:

$$w(R_k, t_a) \approx K' IFFT_{t_a}\left\{|H(f_a, R_k)|^2\right\} \otimes \delta\left(t_a - \frac{X_0}{V_r}\right) \tag{17}$$

The range location R_c can be obtained as (18). Thus the two-dimensional location information of the radiation source can be obtained.

$$R_c = R_k|_{\max(w(R_k,t_a)),t_a=\frac{X_0}{V_r}} \tag{18}$$

The flow of the virtual aperture passive location algorithm is shown in Fig. 4. First, Fourier transform is applied to the acquired signal in the slow time domain. Then estimate the parameters V_r and θ_r of ESRM by geometric approximation and Doppler spectrum. Construct matched filters at different distances, and pass the signal through the matched filters. Reorganize the results by distance and the range location R_c can be obtained by focusing. The radiation source is located at the highest energy.

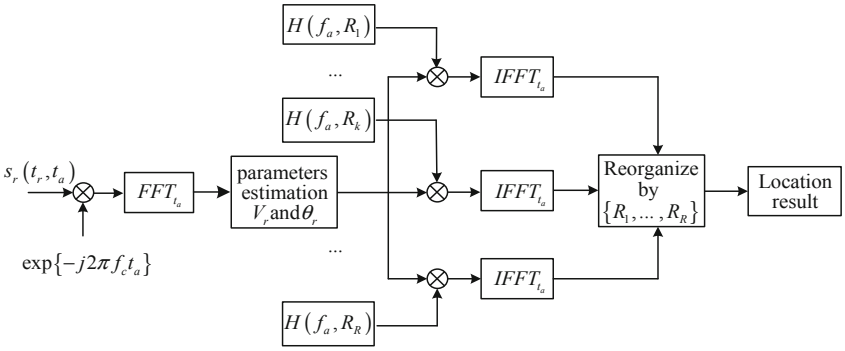

Fig. 4. The flow of the virtual aperture passive location algorithm

4 Resolution and Phase Error of the Range Model

4.1 Azimuth Resolution

The point dispersion function (PSF) determines the azimuth resolution:

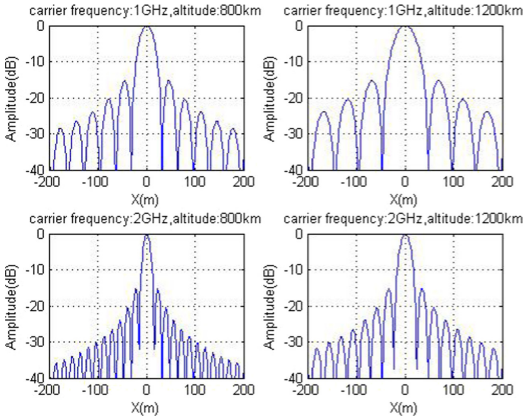

Fig. 5. The PSF in different ranges and frequency

$$psf(t_a, R_k) = IFFT_{t_a}\left\{|H(f_a, R_k)|^2\right\} \tag{19}$$

According to (19), in the case of the same number of samples in the azimuth domain, PSF depends on frequency and range. The graphs of PSF in different ranges and frequency are shown in Fig. 5. As the Fig. 5, it's easy to see that the higher frequency and the closer distance can make higher resolution.

4.2 Range Resolution

The location accuracy in the range domain depends on the distance interval of the set of matched filters. Therefore, to improve the positioning accuracy in the range domain, a step-by-step method can be adopted. First, a larger interval can be used for coarse location, and then a smaller interval around the approximate range can be used for precise location of the radiation source.

4.3 Phase Error of the Range Model

The difference between the range model and the true slant range will cause phase error. The phase error is:

$$\Delta\varphi = -\frac{2\pi}{\lambda}[R(t_a) - R_{true}(t_a)] \tag{20}$$

Analyze the phase error under different orbital altitudes and latitudes, the result is shown in Fig. 6. As Fig. 6, the longer the synthetic aperture time is, the greater the phase error is. When the synthetic aperture time is less than 1 s, the phase error is less than 0.25π.

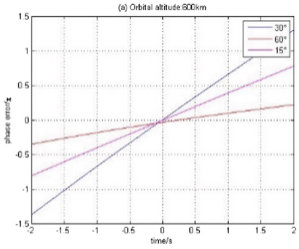

(a)Orbital altitude:600km

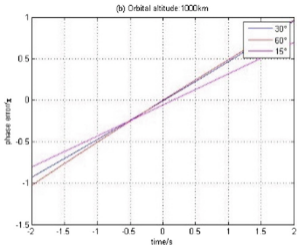

(b)Orbital altitude:1000km

Fig. 6. The phase error curves

5 Simulation

To prove the effectiveness of the algorithm, experiments are conducted. The signal parameters are shown in Table 1. The orbit parameters are shown in Table 2.

Table 1. The signal parameters

Parameters	Values
Carrier frequency	1 GHz
Sampling frequency	30 MHz
Pulse width	10 μs
Pulse repetition frequency (PRF)	5 kHz
Synthetic aperture time	1 s
SNR	0 dB

Table 2. The orbit parameters

Parameters	Values
Orbital altitude	1000 km
Eccentricity	0.0001
Inclination	98°
Argument of perigee	0°
Right ascension of ascending node	105°

The radiation source is located at $(114°\mathrm{W}, 60°\mathrm{N})$. The results are shown in Fig. 7. The received signal is a linear frequency modulation signal in the azimuth, so after azimuth Fourier transform the Doppler spectrum is with a certain width, which is in Fig. 7(a). The location result is shown in Fig. 7(b). By calculation, the error of the method is 1.5 km, which is more accurate than the direction-finding location method based on the phase interferometer.

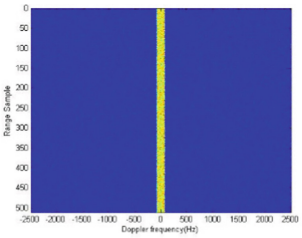

(a) The Doppler spectrum

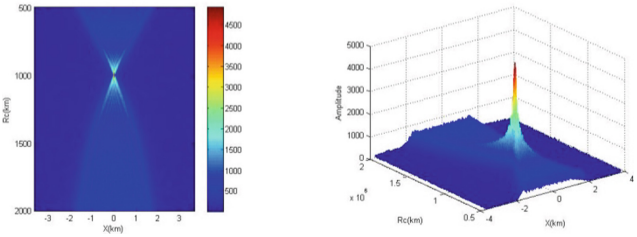

(b) The 2-D location result

Fig. 7. The passive location result

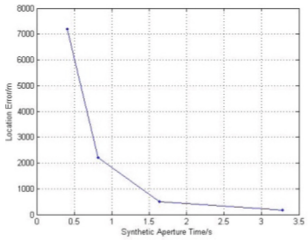

(a) synthetic aperture time-location error curve

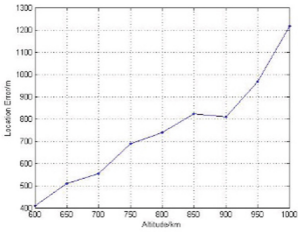

(b) altitude-location error curve

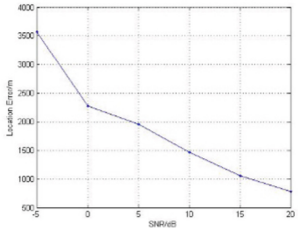

(c) SNR-location error curve

Fig. 8. The location error curves

Then simulate to discuss the factors influencing the accuracy of the location method. Considering the synthetic aperture time, orbital altitude and SNR, the error curves of location are shown in Fig. 8.

It can be seen from Fig. 8 that the location error is decreasing with the longer synthetic aperture time, the lower orbital altitude and the larger SNR.

6 Conclusion

This paper applies the virtual aperture to the space-borne passive location. The proposed method in this paper can obtain radiation source location by range searching and azimuth focusing. The signal model under the Equivalent Squint Range Model was deduced in this paper. The passive location method and the range model parameters estimation method were proposed. Azimuth resolution, range resolution and the error caused by the range model of the method were also deduced in this paper. Simulations were conducted to verify the effectiveness of the method and the factors influencing the location accuracy.

Acknowledgment. This work was supported by the Nation Scient Foundation under grant 62031014.

References

1. Huang, J.H., Barr, M.N., Garry, J.L., Smith, G.E.: Subarray processing for passive radar localization. In: 2017 IEEE Radar Conference, Seattle, WA, pp. 0248–0252 (2017)
2. CongFeng, L., Jinwei, Y., Juan, S.: Direct solution for fixed source location using well-posed TDOA and FDOA measurements. J. Syst. Eng. Electron. **31**, 666–673 (2020)
3. Liu, Z., Wang, R., Zhao, Y.: Computationally efficient TDOA and FDOA estimation algorithm in passive emitter localization. IET Radar Sonar Navig. **13**, 1731–1740 (2019)
4. Shu, F., Yang, S., Lu, J., Li, J.: On impact of Earth constraint on TDOA-based localization performance in passive multi-satellite localization systems. IEEE Syst. J. **12**, 3861–3864 (2018)
5. Dempster, A.G., Cetin, E.: Interference localization for satellite navigation systems. Proc. IEEE **104**, 1318–1326 (2016)
6. Zhu, Y., Zhang, S.: Passive location based on an accurate Doppler measurement by single satellite. In: 2017 IEEE Radar Conference, Seattle, WA, pp. 1424–1427 (2017)
7. Li, T., Guo, F., Jiang, W.: Multiple hypothesis NLS location algorithm based on ambiguous phase difference measured by a rotating interferometer. J. Electron. Inf. Technol. **34**, 956–962 (2012)
8. Kawase, S.: Radio interferometer for geosynchronous-satellite direction finding. IEEE Trans. Aerosp. Electron. Syst. **43**, 443–449 (2007)
9. Yuqi, W.: Passive localization algorithm for radiation source based on long synthetic aperture. J. Radars **9**, 185–194 (2020)
10. Wang, Y., Sun, G., Xiang, J., Xing, M., Guo, L., Yang, J.: A imaging passive localization method for wideband signal based on SAR. In: 2019 6th Asia-Pacific Conference on Synthetic Aperture Radar (APSAR), Xiamen, China, pp. 1–4 (2019)